

Article

A Wireless Electrooculogram (EOG) Wearable Using Conductive Fiber Electrode

Kee S. Moon ^{1,*}, Sung Q. Lee ^{2,*} , John S. Kang ¹ , Andrew Hnat ¹ and Deepa B. Karen ¹¹ Department of Mechanical Engineering, College of Engineering, San Diego State University, San Diego, CA 92182, USA² Future & Basic Technology Research Division, ICT Creative Research Laboratory, Electronics and Telecommunications Research Institute, Daejeon 34129, Republic of Korea

* Correspondence: kmoon@sdsu.edu (K.S.M.); hermann@etri.re.kr (S.Q.L.)

Abstract: Electrooculography (EOG) is a technique for detecting electrical signals from the extra-ocular muscles. The EOG is a precise method for quantifying eye movements, including drowsiness-induced eye closure, and is also a promising technology for its potential use as a contributing mechanism for brain–computer interface applications. Despite the fact that EOG signals change as humans move their eyes, it is still difficult to monitor eye movement patterns in natural behaviors, such as everyday activity. Wearable convenience is essential for obtaining EOG signals while moving freely. This paper proposes the development and use of semi-dry electrodes with low impedance and excellent wearability, as well as a small, portable device with wireless communication capabilities, to increase the likelihood of use in real-life scenarios. The semi-dry electrode produced by the electrospinning technique had an impedance that was 3.5 times lower than that of the existing dry electrode and demonstrated low impedance drift even after long-term use. Furthermore, three steps of eye motion separation were performed using a signal obtained from the wearable device. It was confirmed that the classification of eye movements was at a meaningful level.

Keywords: biopotential electrode; electrooculography; everyday activity



Citation: Moon, K.S.; Lee, S.Q.; Kang, J.S.; Hnat, A.; Karen, D.B. A Wireless Electrooculogram (EOG) Wearable Using Conductive Fiber Electrode. *Electronics* **2023**, *12*, 571. <https://doi.org/10.3390/electronics12030571>

Academic Editor: Enzo Pasquale Scilingo

Received: 2 December 2022

Revised: 17 January 2023

Accepted: 18 January 2023

Published: 23 January 2023



Copyright: © 2023 by the authors. Licensee MDPI, Basel, Switzerland. This article is an open access article distributed under the terms and conditions of the Creative Commons Attribution (CC BY) license (<https://creativecommons.org/licenses/by/4.0/>).

1. Introduction

It has been noted that very little eye movement research over the last century has focused on everyday activities. For example, studies of eye movement during sleepy driving can help to prevent car accidents [1]. Electrooculography (EOG) is one of many methods used to evaluate a person's level of alertness. Eye movement signals help in determining whether a person is sleeping or awake [2,3] However, the real-time characterization of eye movements in natural tasks is still a work in progress. The recent advancement in mobile wireless sensor technology can enable eye tracking in everyday tasks [4].

Wearable convenience is essential for obtaining EOG signals while moving freely. First of all, a low impedance electrode with high signal stability and easy attachment and detachment is an important factor in such convenience. Second, it is necessary to design a sufficiently small and compact device that is comfortable to wear in everyday life.

The voltage can be measured by placing an electrode with a low electric potential between the corneas and retinas of the eyes. EOG is a technique for measuring the retina's action potential. The voltage difference measured between the retina and cornea of the eye is negligible—the resting eye potentials range from 15 V to 50 V. When there is a slight eye movement, the voltage difference can be increased to the micro-volt range [5]. One disadvantage of the EOG system is the placement of the electrodes around the eyes, which can cause discomfort for users. People's EOG signal patterns differ in shape due to individual physiological properties and different ways to move the eyes, as well as skin conductance [6].

The goal of this research is to develop a real-time wearable EOG interface using a novel conductive polymer fiber core electrode fabricated through an electrospinning. One of the most commonly used biopotential electrodes in EOG testing is a wet electrode with adhesive gel embedded in it to improve conductivity between the electrode and the skin. However, because of this gel, applying adhesive-type electrodes to the skin is extremely inconvenient, especially for wearable applications. Dry electrodes with no gel are also available; however, they have limitations in terms of EOG sensitivity. As a result, the purpose of this study was to put prototype semi-dry electrodes to the test. In this paper, we present a semi-dry polymer fiber core electrode with an electrolyte gel impregnated inside the micro-fiber core. The gel-impregnated fiber core is critical in increasing the amount of ion exchange for biopotential signal transduction due to the fiber core's high surface area with a small amount of gel.

In the eye tracking moment, there are two candidates for a sufficiently small compact device at a level that is convenient to wear in daily life. The first is the optical method and the second is the EOG method. Several methods for optically tracking eye movements have been studied and are now widely used in research and commercial applications. These techniques are video-oculography (VOG), video-based infrared (IR), pupil–corneal reflection (PCR), and electrooculography [7]. The term video-oculography refers to the use of a camera-based eye-tracker [8]. A video tracking system requires an unobstructed view of the eye. The reflection of eyeglasses, changing lighting conditions, droopy eyelids, or heavy makeup can all have an impact on tracking quality [8]. An EOG is a technique that detects eye movements by measuring the voltage between two electrodes. An electrooculogram is a system that uses electrodes to measure the potential resting difference between the cornea and retina. However, the potential is extremely small [9]. The vertical and horizontal EOG components are recorded using biopotential electrodes. Vertical eye movement is recorded using EOG up and EOG down, while horizontal eye movement is recorded using EOG right and EOG left. Silver–silver chloride electrodes are the most commonly used electrodes for recording eye movements. A difference in electric potential can result in a difference in dipole positioning, which can be measured to track eye movements [5]. Appendix A Table A1 of the supplement summarizes a brief comparison of the two methods, suggesting An EOG with a semi-dry electrode has a significant advantage over other schemes.

When compared to a video-based eye-tracking system, the EOG system has some advantages. One of them is that it does not require multifaceted video or image processing, and the signal processing is computationally light. Another advantage of the EOG system is that changing the lighting condition only has a minor effect on EOG signals. It can also be measured with the eyes closed or in complete darkness. Because of these factors, the EOG is a well-known measurement method for recording eye movements. Using eye-tracking solutions is also important in cognitive studies, medicine, and psychology. This growing interest in the use of eye-tracking devices, in turn, drives additional advances for new results [10].

In Section 2, the paper describes the electrode design and manufacturing process of a semi-dry electrode with low impedance, high signal stability, and easy attachment and detachment. Section 3 provides an overview of the EOG wearable system, which is a sufficiently small compact device that is comfortable to wear in daily life. Section 4 describes the experimental results and analysis method for monitoring EOG signals. Finally, in the Conclusion Section, we summarize the findings of the study.

2. Electrospun Conductive Biopotential Electrode with Porous Fiber

2.1. Overview of Conductive Biopotential Electrodes

Most currently available electrodes use metallic material in conjunction with an electrolyte gel to drive ion exchange via redox reactions. The majority of biopotential electrodes on the market today are either wet or dry. They either use an adhesive or electrolyte gel, or they rely solely on the geometry of the electrode to make contact with the skin, with no gel

or adhesive. Wet electrodes are heavily reliant on skin abrasion and preparation. Due to their geometry, which incorporates spikes, needles, or bristles to push past the SC layer into the more conductive skin regions, dry electrodes are frequently uncomfortable [11]. The gel used with the wet electrodes aids in lowering the resistance of the skin interface. The main difference in skin interface between typical wet, semi-dry, and dry electrodes is that they either use electrolyte gel or a spiked geometry to create a more conductive skin contact medium [11–15]. However, in this study, conductive polymer materials were investigated and tested as an alternative to performing this ion exchange and transfer.

Carbon graphitization occurs when the material's atoms form a distinct honeycomb lattice structure. Graphene, a single atomic layer of graphite, is a layer of carbon aromatic ring chains [16]. The honeycomb lattice structure of graphene provides excellent structural properties (approximately 200 times stronger than steel), but more importantly in this case, the nature of the carbon bonds in this specialized structure is what gives the plastic its electrically conductive properties [17]. The conductive graphene polymer, in conjunction with the electrolytic gel, could perform a similar function in ion transfer and exchange, which is typically performed by the previously described redox reactions of the silver–silver chloride electrodes. The combination of the conductive nature of the graphene-infused polymer and the highly conductive electrolyte gel could be an excellent substitute for conventional electrode materials. The EOG prototype electrode was made by electrospinning a conductive polymer fiber core. Electro-spinning is a technique used to create micro- or nanofiber materials. Because of their high surface area-to-volume ratio, micro- or nanofibers are desirable materials for many applications [18]. These ratios are made possible by manufacturing fibers ranging in size from micron to nanoscale. Furthermore, the large surface area made possible by the small diameter fibers is beneficial in many processes. Electrospinning is the process of extruding a polymer solution or melted polymer in the presence of a strong electric field. The extruding nozzle of the polymer solution or melt is connected to a positive high-voltage connection from a high-voltage power supply in both cases. When high voltage is applied to the setup, the polymer is extruded at a specific rate, and the electrospinning process begins [19].

2.2. Fabricating Process of Semi-Dry Electrode with Porous Fiber

In this study, the electrode was produced by electrospinning to create a highly porous fiber 'ball' with a large surface area for ion exchange to occur. The concept behind this electrode is to replace the traditional silver–silver chloride sensor core and its redox reactions with a conductive graphene-based polylactic acid (PLA) polymer. As previously stated, the open carbon pi (π) bonds in the graphene sheet that form electron clouds could serve as a substitute for conducting electron transfer for biopotential signal transduction across the skin–electrode interface.

Figure 1 shows the melt electrospinning system setup with a high-voltage power supply and heating element coil used for conductive fiber fabrication [20]. The polymer solution or melt extruding nozzle is attached to a positive high-voltage connection from a high-voltage power supply. A collector basket connects the ground to an aluminum base. When high voltage is applied to the setup, the electrospinning process begins, and the polymer is extruded at a specific rate. A 12-volt lithium–iron–phosphate battery was used to power the heating element, which was wired to the structure's positive and negative terminals. This setup made use of an Acopian P030HA2 power supply, which is voltage-adjustable and has a maximum output of 10 kV. An alligator clamp was used to secure the high-voltage positive lead to the nozzle of the electrospinning setup. Another alligator clip was used to connect the negative lead to the aluminum foil collector plate sheet. The nozzle-collector distance was set at 150 mm to allow the polymer fiber to perform the electrospinning whipping motion without colliding with the negative plate and short-circuiting. The temperature at which the polymer melt was extruded was 230 °C, as measured and confirmed by an infrared laser thermometer. A higher nozzle temperature was found to help reduce the viscosity of the polymer melt and create more pressure within

the nozzle, causing the molten plastic to jet out of the nozzle at a much faster rate at the Taylor cone. As the plastic was extruded into the electric field at a lower viscosity but at a higher pressure, smaller pieces of extruded fiber experienced the whipping motion phenomenon, in which the whipping motion appeared to pull and draw down the molten polymer fiber into a noticeably smaller diameter. This success in fiber production prompted more tinkering with some of the parameters, most notably the applied voltage, in order to optimize the fiber size. The final resulting input voltage used to induce the electric field for electrospinning of the conductive polymer fiber was 3.2 kV, as measured with an industrial multimeter.

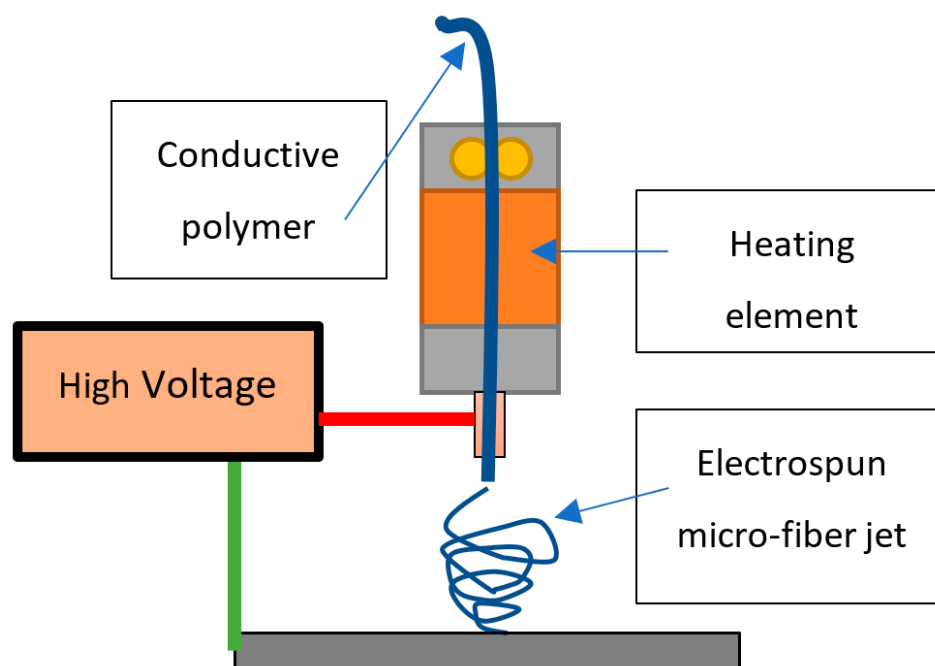


Figure 1. Melt electrospinning system setup with a high-voltage power supply and heating element coil.

In this study, we created and tested an experimental electrode that is a hybrid, semi-dry design that falls somewhere between the two main types of dry and wet electrodes currently used in healthcare. The impedance should be reduced significantly by increasing the surface contact area by filling in the microfibers. The dry electrode, on the other hand, relies solely on the spikes to make contact with the skin. Figure 2 shows a SEM image of a successful electrospun fiber formation. This study made use of a tabletop Hitachi TM3000 SEM. It depicts four different SEM captures of the fiber network on the second prototype electrode's fiber core at magnifications of $60\times$, $120\times$, $200\times$, and $400\times$. The figure shows that the electrospinning process produced human hair-like conductive polymer fibers.

2.3. Impedance Analysis of Semi-Dry Electrode

At the forefront of modern technology is research on flexible electrodes with low skin contact resistance, with graphene being a prime example. Their skin contact resistance is reported to be between $500\text{ kohm}@100\text{ Hz}$ and $68\text{ kHz}@10\text{ Hz}$, and they are aiming for low skin contact resistance [21]. Table 1 compares the electrodes developed in this study to commercial products to assess impedance, a key performance of electrodes. An impedance analysis showed that, on average, the fiber core electrode had the same or lower impedance as industry-standard ECG electrodes. Lower impedance and equivalent circuit values indicate clearer signal transduction between the skin–electrode interface, resulting in more explicit EOG recordings. In Table 1, all of the measurements were taken five times to obtain an average, and the standard deviation of the measured impedance in each case was between 5% and 10% of the average value. When compared to the 3M adhesive electrode,

the data set from the semi-dry fiber-PLA showed a 50% improvement using 1.0 mL of gel at both 50 Hz and 250 Hz. Furthermore, the data set from the semi-dry fiber-PLA at 50 Hz showed a 70% improvement using 1.0 mL of gel compared to the semi-dry fiber-PLA electrode with 0.1 mL of gel. The results also demonstrate how important the gel is for the successful operation of the second prototype semi-wet fiber core electrode. The gel is essential for filling voids within the fiber core and allowing ion exchange between the skin, gel, and polymer for a good connection and signal read-out. The tests also show that the prototype electrospun fiber core electrode requires a small amount of electrolyte gel to saturate the entire fiber core of the electrode for clearer signal transduction. Only the skin end of the electrode core could be impregnated with less gel. The increased surface area of the electrospun fiber core combined with the conductive electrolytic gel was found to have a high sensitivity in transducing biopotential signals. A series of trials were performed to analyze the impedance of each electrode over a range of frequencies using an Agilent 4294a impedance analyzer (40–110 MHz, Agilent, Santa Clara, CA, USA).

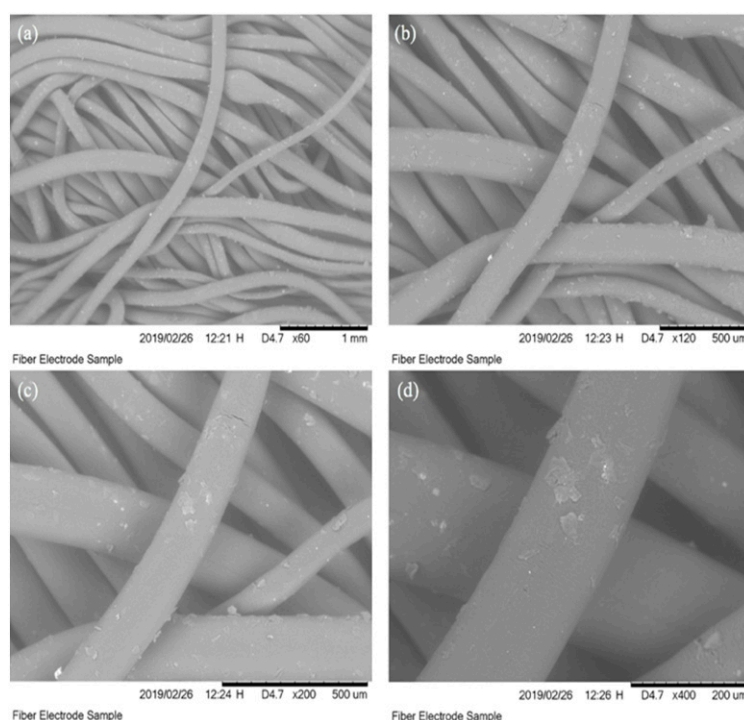


Figure 2. Scanning electron microscope (SEM) images of the porous electrospun fiber network at various magnifications. (a) 60 \times , (b) 120 \times , (c) 200 \times , and (d) 400 \times .

Table 1. The impedance comparison of manufactured samples with other commercials.

Specification (CASE)	Impedance * (50 Hz, k Ω)	Impedance * (250 Hz, k Ω)	Value	Comments
A: wet adhesive-AgCl	74.218	47.895	Wet	Commercially available (3M)
B: dry spiked-AgCl	108.453	87.053	Dry	Commercially available (OPENBCI)
C: semi-dry fiber-PLA	121.274	77.552	Semi-dry: 0.1 mL of gel	Proposed
D: semi-dry fiber-PLA	36.882	23.638	Semi-dry: 1.0 mL of gel	Proposed
E: dry Graphene on Polymer	~500	-	Flexible, 60 times reuse	(ref) ACS Appl. Nano Mater. 2022, 5, 8, 10137–10150 [21]

* Average of 5 measurements.

A 15-min impedance drift test was also included to measure the impedance characteristics of the electrodes [22]. Table 2 compares the impedance drift, which can be a problem in everyday life: sensitivity changes as impedance increases, and the proposed

electrode showed a relatively small drift. Table 2 and Figure 3 show that the impedance of most electrodes remained relatively stable and varied by less than one-tenth of $k\Omega$. The promising results of the in-lab developed electrodes have demonstrated a strong potential for a new design of biopotential sensors to be investigated for designing an EOG wearable interface without the use of conventional sticky electrodes.

Table 2. The impedance drifts of the test samples (15-min measurements at 50 kHz).

Specification (CASE)	Mean ($k\Omega$)	Standard Deviation ($k\Omega$)	Total Change ($k\Omega$)
A: wet adhesive-AgCl	0.321	0.187	0.005
B: dry spiked-AgCl	1.944	0.053	0.177
D: semi-dry fiber-PLA	0.254	0.001	0.002

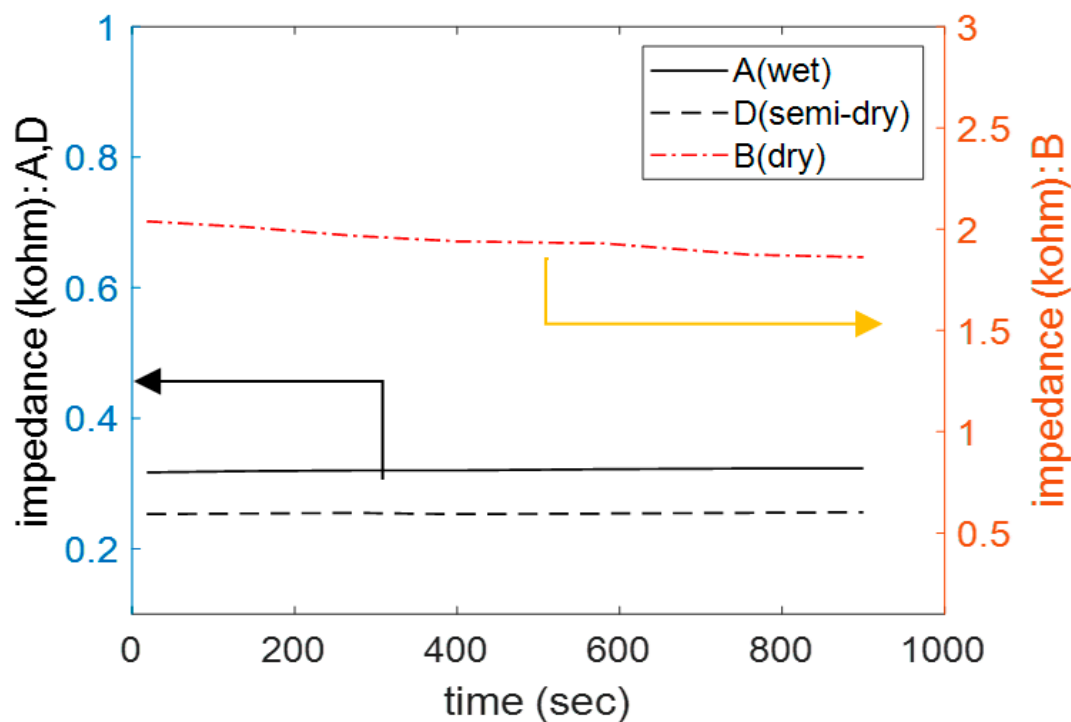


Figure 3. The impedance drifts of the test samples (15-min measurements at 50 kHz).

3. EOG Experimental Setup and Results

3.1. Wireless EOG Device for Wearable Applications

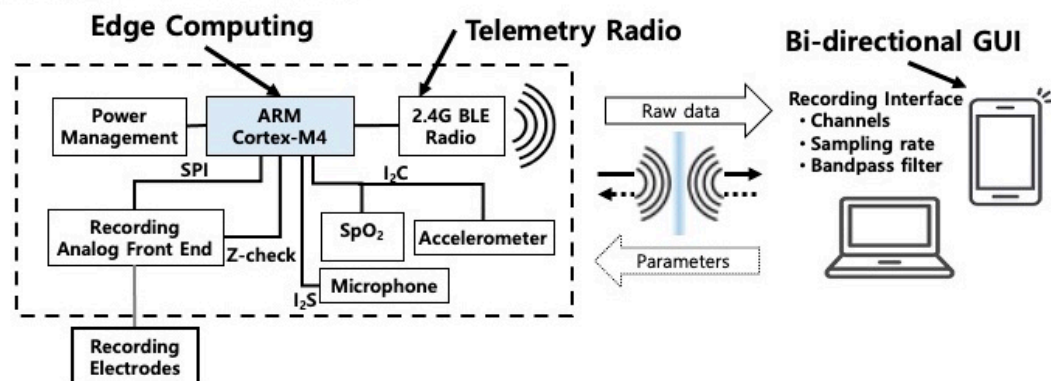
It is critical to configure a sufficiently small compact device that is comfortable to wear in daily life. Figure 4 shows a wireless wearable EOG sensor that can remotely monitor and record the EOG biopotential signals of the eye movements onto their computing system for further visualization and analysis. The wearable sensor system includes sensor electrodes, a data acquisition and signal-processing circuit, and a wireless data transmission chip. The transmitted signals are analyzed in real time by an external computer system.

As shown in Figure 4, EOG detection is accomplished by placing a pair of semi-dry electrodes mounted on a small headphone on the sides of the eyes (c). In the wearable, the electrodes convert eye movements into analog electrical signals. Furthermore, the system can wirelessly transmit signals up to 10 m to a remote processing network, promoting potential assistive driving applications. It also allows for automatic interpretation in drowsiness diagnostics.

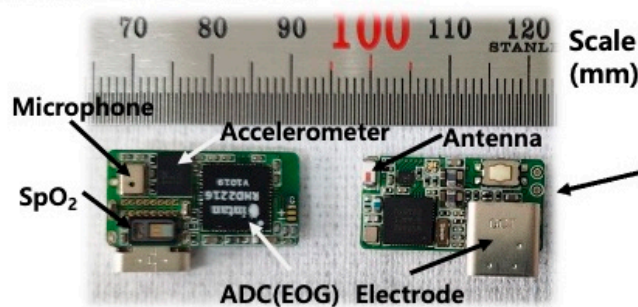
The digital electrophysiology interface chips from Intan Technologies, LLC (Los Angeles, CA, USA) are used for the signal acquisition module. The RHD2216 chip, a low-power 16-channel differential amplifier integrated with a 16-bit analog-to-digital converter (ADC), was used to record the EOG. Because of its low power consumption and flexibility, we chose

the Nordic Semiconductor nRF52832 System-on-Chip (SoC) for computing and wireless data transmission on the module. It is based on an ARM cortex-M4 processor with a 64 MHz clock and single-cycle multiply and accumulate (MAC) instructions. Furthermore, the processor's single-precision floating-point unit (FPU) is suitable for real-time analysis of the incoming neural signals. We designed the device to call the interrupt service routine (ISR) at 4096 Hz from a crystal oscillator at 32,768 Hz, resulting in a sampling frequency of 4.096 kHz. The wearable interface communicates wirelessly with a local external computer via BLE technology, where the signal data is processed and classified in real-time using a custom executable C program. Table 3 contains detailed descriptions of the wireless EOG device components, as well as their specifications.

(a) Block diagram of wearable EOG



(b) Wearable EOG Hardware



(c) Wearable EOG setup

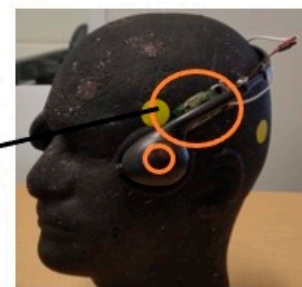


Figure 4. Overall system block diagram of the wireless EOG device.

Table 3. The specifications of the wireless wearable EOG interface.

Specification	Description	Value
EOG sensor circuit size	PCB & battery	(30 × 10 × 3) mm
Power source	Rechargeable battery	8 h/charging
Data transmission	Bluetooth wireless	1M bps in 2 m
EOG electrodes	Reusable semi-dry micro-fiber core	5 mm diameter
Front-end circuit	Intan Tech Chip	10 mV, 16 bit, 1 ch
Onboard CPU	ARM Cortex M4	4096 Hz/ch sampling rate
Wireless circuit	NRF 52X	2.4 G ESB RF

In this study, we performed a feasibility experiment with a standard commercial wired five-electrode and wearable setup for comparison (Figure 5). The experiment was carried out in a lab setting using commercial instrumentation in this step. To obtain accurate standard EOG signals, a subject was seated in front of a computer screen at a distance of 60 cm and was not allowed to move the upper body or head during the experiment.

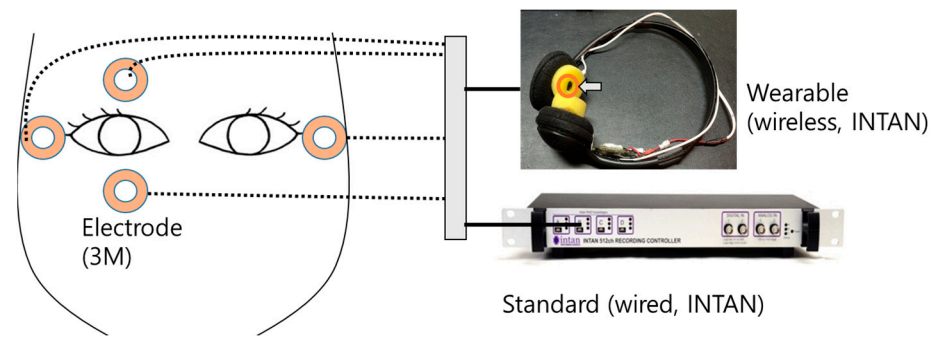
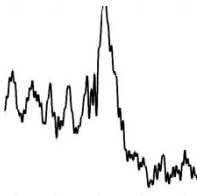

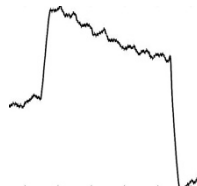



Figure 5. EOG recording standard and wearable with 3M disposable ECG electrode patches.

The commercial 3M disposable ECG electrode patches were attached around the eyes in both the wearable and standard recordings (Figure 5). The eye movement signal data was recorded using a commercial INTAN 512 channels recording controller (Intan Technologies, Los Angeles, CA, USA) in the standard recording, and we used a wireless EOG device developed in this study in the wearable recording. Table 4 describes the two types of EOG patterns. The EOG patterns in the “wearable” column show that the proposed wearable EOG interface provides an EOG signal quality comparable to the standard wired EOG method.

Table 4. The verification experimental results.

Eye Motion Pattern	Wearable *	Standard **
Blinks		
Horizontals		

* Wearable: the EOG raw signals from the EOG system with the electrospun electrodes. ** Standard: the EOG raw signals from of the INTAN recorder.

3.2. Single Eye Movements Discrimination

The EOG experimental study to detect typical eye movements is described in this section. All of the experiments were carried out with the subject sitting. The study collected a set of experimental sensor signals from a healthy individual who is also one of the authors. The two types of EOG patterns produced by a single channel EOG system with electrospun electrodes were attached to a commercial headset.

The purpose of this study is to show the feasibility of using a new approach of using semi-dry conductive fiber core electrodes to generate a visual EOG pattern with a wire-free wearable interface. The following three common eye movements were used in an experimental study to detect eye movements: “rest”, “horizontal,” and “blink”. For the EOG experiment, only two electrodes were placed around the eye region. Figures 6–8 show the time and amplitude characteristics of typical EOG signals obtained from blinking, resting, and left–right movement at the side of the eye. Figure 6 depicts the detection of the peaks of each absolute peak of the EOG signals. Figure 7 also shows that there is clear

evidence of decreased intervals between each peak of the EOG signals at the measuring location. Figure 8 shows that the interval increases in horizontal movement.

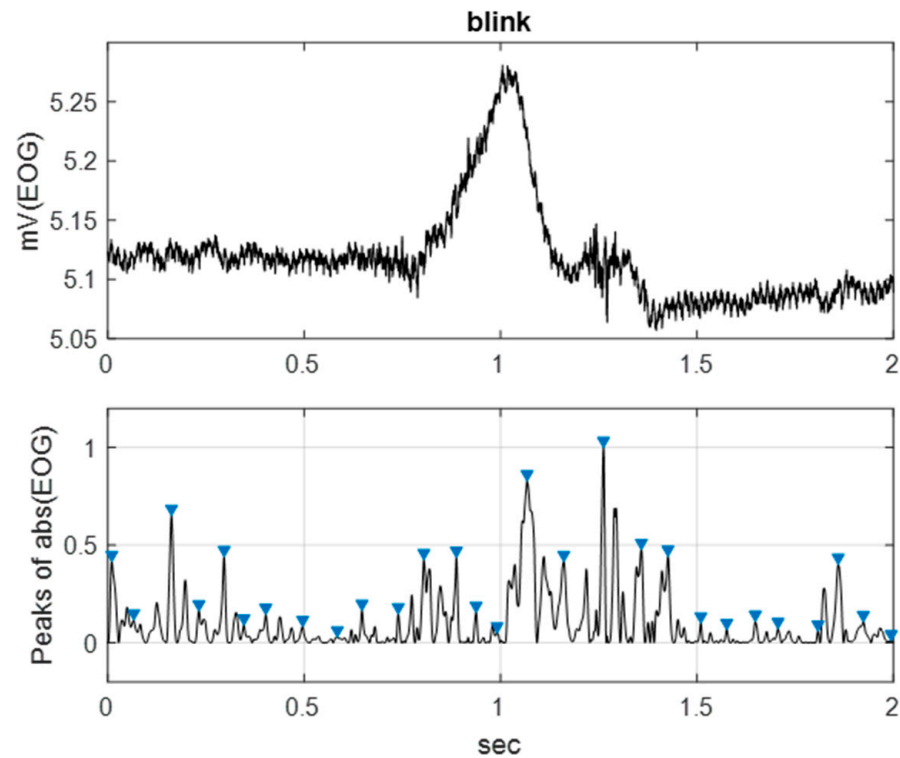


Figure 6. The EOG pattern of “blink” eye movement from one channel EOG system with the electrospun electrodes assembled on a headset. (y-axis unit: a normalized value of millivolt).

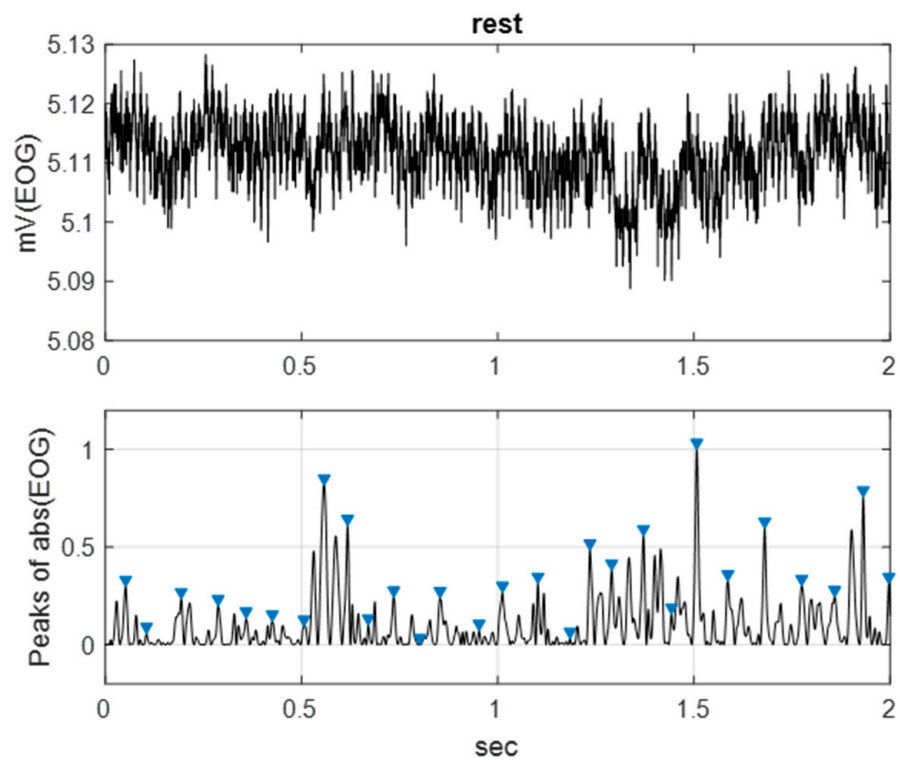


Figure 7. The EOG pattern of “rest” eye movement from one channel EOG system with the electrospun electrodes assembled on a headset. (y-axis unit: a normalized value of millivolt).

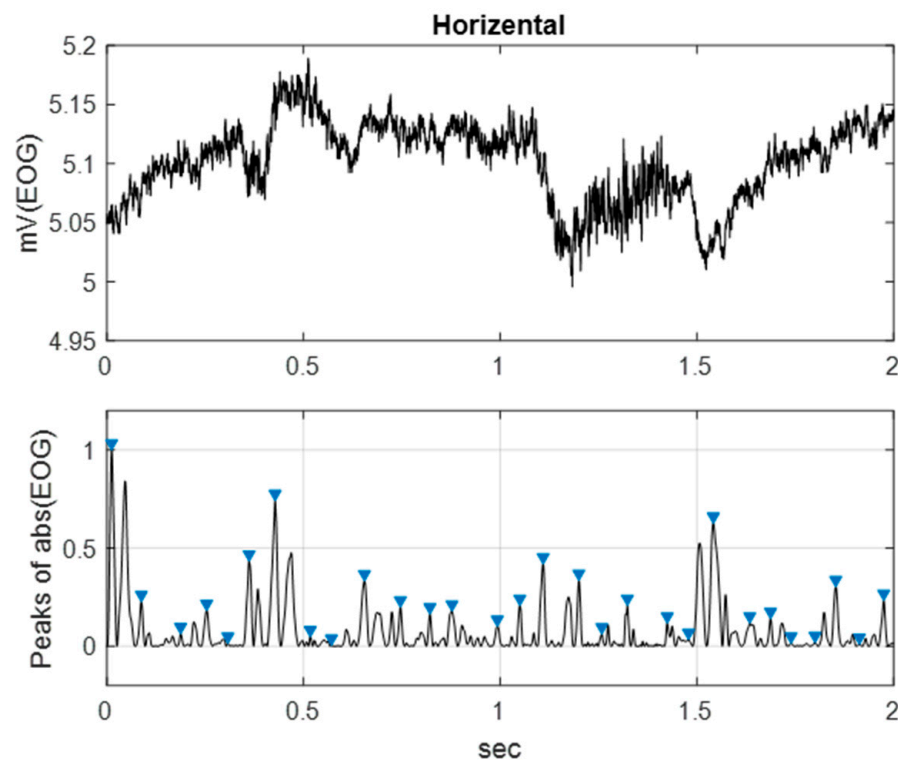


Figure 8. The EOG pattern of “horizontal” eye movement from one channel EOG system with the electrospun electrodes assembled on a headset. (y-axis unit: a normalized value of millivolt).

In this paper, we present two new indices for estimating the EOG signal’s characteristic changes for our wearable interface. As a first index, we define the eye beat rate (EBR) as the number of low-frequency beats per minute, as shown in Figures 6–8.

The i -th each successive time difference between the two beats x_i in the low-frequency eye beat cycles is calculated as:

$$x_i = t_n - t_{n-1} \quad (1)$$

where t_n denotes the inter-beat interval of the n -th peak in the signal.

$$EBR = [(\sum_{i=1,N} x_i) / N]^{-1} \quad (2)$$

where N denotes the total number inter-beat intervals in the signal per unit period.

As a second index, the eye beat rate variability (EBRV) is defined as the root mean square of successive differences between eye beats that are obtained by first calculating each successive time difference between the beats in ms (x_i) from Equation (1). Then, each of the values of x_i is squared and averaged. We expect the EBRV reflects the time-domain index used to estimate the short-term EOG signal changes.

$$EBRV = \sqrt{\frac{1}{N} \sum_{i=1,N} x_i^2} \quad (3)$$

The EBRV measures eye movement function and could be caused by eye–brain interactions, though more research is needed in the future. Furthermore, the EBRV can be used as an index to help us monitor sleepiness while driving. Table 5 and Figure 9 show the EBR and EBRV indices in each eye movement pattern. It is notable that the EBR and EBRV are effective indices for classifying eye motion. In the two indices, EBR showed a clear difference in distinguishing whether the eye moves, and EBRV can clearly distinguish whether the eye moves or not, but also beyond a significant margin of error in distinguishing whether the eye blinks or moves left and right. This suggests that simple indices of single-channel EOG could be useful in studies of automated eye movement characterization. Previously, discrete wavelet transform (DWT), refined composite multiscale

dispersion entropy (RCMDE), and the autoregressive (AR) model, for example, were used to analyze single channel EOG signals [3]. However, the proposed method of computing *EBR* and *EBRV* has the advantage of analyzing and selecting features in real time due to the small data size.

Table 5. The outcomes of the wireless wearable EOG interface. (2 s time period, 6-sample average).

Eye Motion Patterns	<i>EBR</i> (per min)	<i>EBRV</i> (ms)
"rest"	882	18
"blink"	814	25
"horizontal"	801	28

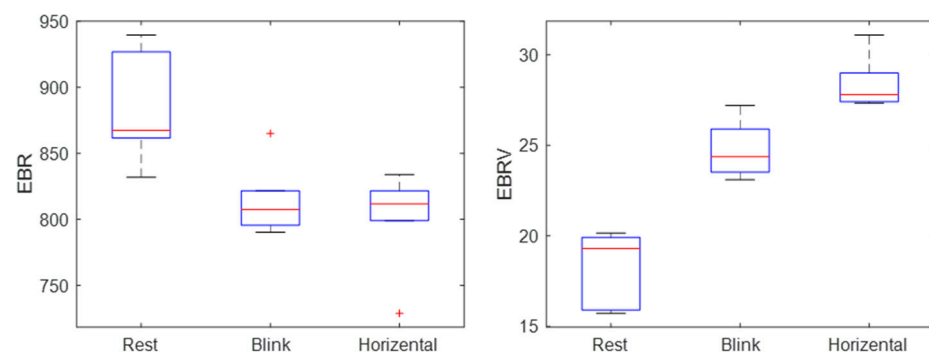


Figure 9. Eye movement classification using the wearable EOG.

4. Conclusions

Previous applications of EOG have been limited because EOG signals are obtained by placing five electrodes around both eyes to record eye movements. As a result, most EOG applications have been limited to the medical field of diagnosis, such as child development, sleep studies, and other areas. In this study, we proposed a wireless wearable EOG interface for monitoring eye movements with reasonable accuracy using novel semi-dry conductive fiber core electrodes.

The prototype electrode was a semi-dry design that made use of a conductive polymer and an electrolytic gel made from electrospun fibers. The results of static and long-term drift impedance analysis tests revealed that, on average, the conductive polymer fiber core electrode exhibited equal or lower impedance values than standard wet-type electrodes. The application of a thin layer of conductive gel on the surface of this electrode creates an ionic conducting route for the purpose of sensing eye movement signals. The advantage is that it outperforms dry electrodes while eliminating the need for routine disposal of wet electrodes.

The *ERB* and *ERBV* indices are proposed to classify eye motion through offline calculation from the EOG data that was simply measured and wirelessly transmitted to the PC using the BLE communication protocol. In a future study, we will use Arm Cortex, which is built into this wearable EOG, to calculate *ERB* and *ERBV* in real time and process eye motion discrimination instantly. This method is expected to benefit from the convenience of wearing while also being advantageous in terms of power consumption due to real-time onboard computing.

The developed EOG interface and classification indices presented here are useful tools for automatically detecting and analyzing eye movements. It is simple to apply to specific eye movements in daily activities. Please keep in mind, however, that the author only conducted our human study due to the IRB under the COVID-19 pandemic. The EOG wearable interface, we believe, will benefit eye-tracking studies in a variety of disciplines, including physiology, human factors, and assistive driving. More participants can be recruited in the future to see if the EOG interface works well for all people in natural environments.

Surprisingly, we discovered a small clue that our device can be used in human–computer interface (HCI) research [23]. Figure 10 represents the EOG signals obtained from the left–right side of the eye location, with the first 2-s representing the “blink” phase (shown in an orange box) and the following 2-s representing the “rest” phase. It is clear that the low- (EOG-alpha) and high- (EOG-beta) frequency filtered “blink” and “rest” phases can be monitored concurrently. In the future, we will improve eye motion classification by using EOG signals, as well as filtered EOG-alpha and EOG-beta.

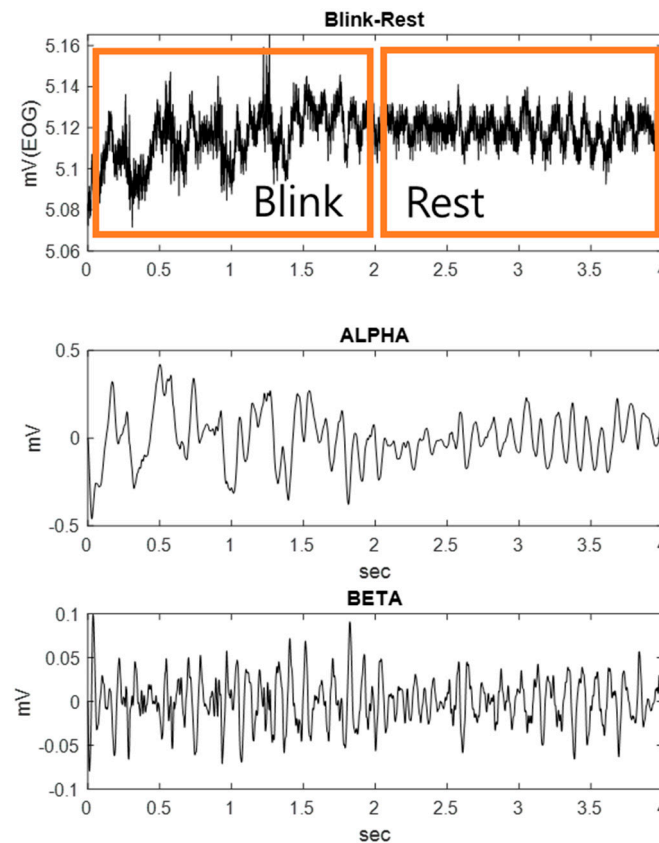


Figure 10. The one channel EOG contains EEG information: alpha and beta waves can be driven to match eye motion.

Author Contributions: Conceptualization, K.S.M. and S.Q.L.; methodology, K.S.M., J.S.K. and S.Q.L.; software, K.S.M. and S.Q.L.; validation, K.S.M.; formal analysis, K.S.M., A.H., D.B.K. and S.Q.L.; investigation, K.S.M.; resources, K.S.M. and S.Q.L.; data curation, K.S.M., A.H., D.B.K. and S.Q.L.; writing—original draft preparation, K.S.M., A.H., D.B.K. and S.Q.L.; writing—review and editing, K.S.M. and S.Q.L.; visualization, K.S.M., A.H., D.B.K. and S.Q.L.; supervision, K.S.M.; project administration, K.S.M.; funding acquisition, K.S.M. and S.Q.L. All authors have read and agreed to the published version of the manuscript.

Funding: This work was partially supported by the SDSU Big Idea grant and the Electronics and Telecommunications Research Institute grant funded by the Korean government (22ZB1160, Neuromorphic decoder–encoder technology and 22YB1200, Collective Brain–Behavioral Modelling in Socially Interacting Group).

Institutional Review Board Statement: Not applicable.

Informed Consent Statement: Not applicable.

Data Availability Statement: Not applicable.

Acknowledgments: The authors would like to thank the SDSU Big Idea team and the Smart Health Institute for their kind support.

Conflicts of Interest: The authors declare no conflict of interest.

Appendix A

Various methods have been investigated to track eye movements. An EOG with a semi-dry electrode is a method that has more advantage over other schemes. It measures the voltage between two electrodes and detects eye movements so that it is robust to environmental conditions, such as light. Semi-dry electrodes provide less impedance and longer recording time merits.

Table A1. Wearable eye movement tracking scheme comparison.

Scheme	Details	Advantage	Disadvantage
VOG (Video-oculography)	Detect capturing eye motion	Direct eye tracking	Varying light conditions Droopy eyelids, Heavy image processing
VOG (Video based IR)	Capturing black area of the pupil by illuminating IR	Direct eye tracking Robust to light environment	Droopy eyelids, Heavy power consumption Hard to wear (heavy equipment)
EOG (Dry electrode)	Bio potential measurement	Wearable (by wireless) Low power consumption Robust to light environment	High contact impedance (weak to noise)
EOG (Wet electrode)	Bio potential measurement	Wearable (by wireless) Low power consumption Low contact impedance	Short time recording Uncomfortable using gel
EOG (Semi-dry electrode)	Bio potential measurement	Wearable (by wireless) Low power consumption Low contact impedance Long time recording	Indirect eye tracking

References

1. NHTSA. Driving. (United States Department of Transportation). Retrieved 2022. 2022. Available online: <https://www.nhtsa.gov/risky-driving/drowsy-driving> (accessed on 31 August 2022).
2. Meng, Q.; Tan, X.; Jiang, C.; Xiong, Y.; Yan, B.; Zhang, J. Tracking Eye Movements During Sleep in Mice. *Front. Neurosci.* **2021**, *15*, 616760. [CrossRef] [PubMed]
3. Rahman, M.M.; Bhuiyan, M.I.H.; Hassan, A.R. Sleep stage classification using single-channel EOG. *Comput. Biol. Med.* **2018**, *1*, 211–220. [CrossRef] [PubMed]
4. Land, M.F.; Hayhoe, M. In what ways do eye movements contribute to everyday activities? *Vis. Res.* **2001**, *41*, 3559–3565, Retrieved 20 September 2022. Available online: <https://www.bankrate.com/insurance/car/drowsy-driving-statistics/> (accessed on 31 August 2022). [CrossRef] [PubMed]
5. Jia, Y.; Tyler, C.W. Measurement of saccadic eye movements by electrooculography for simultaneous EEG recording. *Behav. Res. Methods* **2019**, *51*, 2139–2151. [CrossRef] [PubMed]
6. Dziedzickis, A.; Kaklauskas, A.; Bucinskas, V. Human Emotion Recognition: Review of Sensors and Methods. *Sensors* **2020**, *20*, 592. [CrossRef] [PubMed]
7. Luo, W.; Cao, J.; Ishikawa, K.; Ju, D. A Human-Computer Control System Based on Intelligent Recognition of Eye Movements and Its Application in Wheelchair Driving. *Multimodal Technol. Interact.* **2021**, *5*, 50. [CrossRef]
8. Levo, H.; Aalto, H.; Hirvonen, T.P. Nystagmus measured with video-oculography: Methodological aspects and normative data. *ORL* **2004**, *66*, 101–104. [CrossRef] [PubMed]
9. Creel, D.J. The electrooculogram. *Handb. Clin. Neurol.* **2019**, *160*, 495–499. [PubMed]
10. Martinez-Marquez, D.; Pingali, S.; Panuwatwanich, K.; Stewart, R.A.; Mohamed, S. Application of Eye Tracking Technology in Aviation, Maritime, and Construction Industries: A Systematic Review. *Sensors* **2021**, *21*, 4289. [CrossRef] [PubMed]
11. Yazicioglu, R.F.; Van Hoof, C.; Puers, R. *Biopotential Readout Circuits for Portable Acquisition Systems*; Springer: Dordrech, The Netherlands, 2008.
12. Faisal, S.N.; Amjadipour, M.; Izzo, K.; Singer, J.A.; Bendavid, A.; Lin, C.-T.; Iacopi, F. Non-invasive on-skin sensors for brain machine interfaces with epitaxial graphene. *J. Neural Eng.* **2021**, *18*, 066035. [CrossRef] [PubMed]
13. Li, G.-L.; Wu, J.-T.; Xia, Y.-H.; He, Q.-G.; Jin, H.-G. Review of semi-dry electrodes for EEG recording. *J. Neural Eng.* **2020**, *17*, 051004. [CrossRef] [PubMed]
14. Liu, J.; Lin, S.; Li, W.; Zhao, Y.; Liu, D.; He, Z.; Wang, D.; Lei, M.; Hong, B.; Wu, H. Ten-Hour Stable Noninvasive Brain-Computer Interface Realized by Semidry Hydrogel-Based Electrodes. *Research* **2022**, *2022*, 9830457. [CrossRef] [PubMed]

15. Huang, Z.; Zhou, Z.; Zeng, J.; Lin, S.; Wu, H. Flexible electrodes for non-invasive brain–computer interfaces: A perspective. *APL Mater.* **2022**, *10*, 090901. [CrossRef]
16. de la Fuente, J. Properties of Graphene. Retrieved 29 August 2019. 2022. Available online: <https://www.graphenea.com/pages/graphene-properties#.XIs2Bi2ZOU4> (accessed on 31 August 2022).
17. Nixor. The World of Graphene—Nixor. Retrieved 29 August 2019. 2022. Available online: <https://www.nixor.co.uk/the-world-of-graphene/> (accessed on 31 August 2022).
18. Park, J.S. Electrospinning and its Applications. *Adv. Nat. Sci. Nanosci. Nanotechnol.* **2010**, *1*, 043002. [CrossRef]
19. Li, Z.; Yuan, Y.; Chen, B.; Liu, Y.; Nie, J.; Ma, G. Photo and Thermal Cured Silicon-Containing Diethynylbenzene Fibers via Melt Electrospinning with Enhanced Thermal Stability. *J. Polym. Sci. Part A Polym. Chem.* **2017**, *55*, 2815–2823. [CrossRef]
20. Braiek, M.; Sapountzi, E.; Chateaux, J.F.; Vocanson, F.; Lagarde, F.; Maaref, A.; Jaffrezic-Renault, N. Impedimetric Biosensor Based on Electrospun PEI/PVA Decorated with Gold Nanoparticles for Glucose Detection. *J. Electrochem. Soc.* **2015**, *162*, B275–B281.
21. Faisal, S.N.; Iacopi, F. Thin-Film Electrodes Based on Two-Dimensional Nanomaterials for Neural Interfaces. *ACS Appl. Nano Mater.* **2022**, *5*, 10137–10150. [CrossRef]
22. Li, G.; Wang, S.; Duan, Y.Y. Towards conductive-gel-free electrodes: Understanding the wet electrode, semi-dry electrode and dry electrode-skin interface impedance using electrochemical impedance spectroscopy fitting. *Sens. Actuators B Chem.* **2018**, *277*, 250–260. [CrossRef]
23. Bissoli, A.; Lavino-Junior, D.; Sime, M.; Encarnação, L.; Bastos-Filho, T. A Human-Machine Interface Based on Eye Tracking for Controlling and Monitoring a Smart Home Using the Internet of Things. *Sensors* **2019**, *19*, 859. [CrossRef] [PubMed]

Disclaimer/Publisher’s Note: The statements, opinions and data contained in all publications are solely those of the individual author(s) and contributor(s) and not of MDPI and/or the editor(s). MDPI and/or the editor(s) disclaim responsibility for any injury to people or property resulting from any ideas, methods, instructions or products referred to in the content.